




Article

Monitoring the Vertical Distribution of Maize Canopy Chlorophyll Content Based on Multi-Angular Spectral Data

Bin Wu ^{1,2} , Huichun Ye ^{1,3} , Wenjiang Huang ^{1,3,*}, Hongye Wang ⁴, Peilei Luo ¹, Yu Ren ^{1,2}  and Weiping Kong ⁵

¹ Key Laboratory of Digital Earth Science, Aerospace Information Research Institute, Chinese Academy of Sciences, Beijing 100094, China; wubin2017@radi.ac.cn (B.W.); yehc@aircas.ac.cn (H.Y.); luopl@aircas.ac.cn (P.L.); renyu@aircas.ac.cn (Y.R.)

² University of Chinese Academy of Sciences, Beijing 100190, China

³ Key Laboratory for Earth Observation of Hainan Province, Sanya 572029, China

⁴ Cultivated Land Quality Monitoring and Protection Center, Ministry of Agriculture and Rural Affairs, Beijing 100125, China; xbwang2020@cau.edu.cn

⁵ Key Laboratory of Quantitative Remote Sensing Information Technology, Aerospace Information Research Institute, Chinese Academy of Sciences, Beijing 100094, China; kongwp@aircas.ac.cn

* Correspondence: huangwj@aircas.ac.cn; Tel.: +86-10-8217-8169

Abstract: Remote sensing approaches have several advantages over traditional methods in determining information on physical and chemical parameters, including timely data acquisition, low costs, and wide coverage. Thus, remote sensing is widely used in crop growth monitoring. Unlike vertical observations, multi-angular remote sensing technology can obtain the vertical distribution information of the central and lower leaves of a crop. Furthermore, applications of remote sensing on the vertical distribution of maize canopy components is complicated, and related research is limited. In the current paper, we employed multi-angular spectral data, measured by a self-designed multi-angular observation instrument at view zenith angles (VZAs) of 0°, 10°, 20°, 30°, 40°, 50°, and 60°, to explore the monitoring strategy and monitoring precision of the vertical distribution of chlorophyll content in the maize canopy. This was then used to determine the optimal monitoring method for the chlorophyll content (soil and plant analyzer development (SPAD) value) of each layer. The correlation between SPAD value and chlorophyll sensitivity indices at different growth stages was used as the basis for screening indices and VZAs. The correlation between the selected EPI (eucalyptus pigment index) and REIP (red edge inflection point) indices and chlorophyll content indicated view zenith angles (VZAs) of 0°, 30°, and 40° as optimal for the early growth stage monitoring of chlorophyll content in the 1st, 2nd, and 3rd layers, respectively. These values were associated with RMSEs of 4.14, 1.71, and 1.11 for EPI, respectively; and 4.61, 2.31, and 1.00 for REIP, respectively. In addition, a VZA of 50° was selected to monitor the chlorophyll content of the 1st, 2nd, 3rd, and 4th layers at the late growth stage, with RMSE values of 2.97, 3.50, 2.80, and 4.80 for EPI, respectively; and 3.16, 5.02, 4.55, and 7.85 for REIP, respectively. The results demonstrated the ability of canopy multi-angular spectral reflectance to accurately estimate the maize canopy chlorophyll content vertical distribution, with the VZAs of different vertical layers varying between the early and late growth stages.

Keywords: vertical profile; leaf chlorophyll content; multi-angular off-nadir spectral reflectance; canopy depth detection; maize



Citation: Wu, B.; Ye, H.; Huang, W.; Wang, H.; Luo, P.; Ren, Y.; Kong, W. Monitoring the Vertical Distribution of Maize Canopy Chlorophyll Content Based on Multi-Angular Spectral Data. *Remote Sens.* **2021**, *13*, 987. <https://doi.org/10.3390/rs13050987>

Academic Editor: Frédéric Cointault

Received: 21 January 2021

Accepted: 2 March 2021

Published: 5 March 2021

Publisher's Note: MDPI stays neutral with regard to jurisdictional claims in published maps and institutional affiliations.



Copyright: © 2021 by the authors. Licensee MDPI, Basel, Switzerland. This article is an open access article distributed under the terms and conditions of the Creative Commons Attribution (CC BY) license (<https://creativecommons.org/licenses/by/4.0/>).

1. Introduction

The chlorophyll content of the crop canopy is vertically distributed and exhibits a certain level of stratification. This vertical distribution is of great significance for accurate crop growth monitoring and management. As nitrogen is able to move within the plant

with ease, the chlorophyll in the old leaves will transfer to the new leaves in nitrogen-deficient crops. In particular, chlorosis will initially occur in the lower leaves of the plant and gradually expand to the upper leaves, causing nutrient deficiency in the upper leaves. If the growth status of the middle and lower crop layers is determined at an early stage, early management can be effectively implemented [1]. Several studies on plant nutrition have reported the heterogeneity of canopy chlorophyll content [2,3]. The vegetation index method is one of the most simple and widely used methods in the remote sensing quantitative inversion of vegetation physiological and biochemical parameters. Due to the high reflectivity of green plants due to the strong absorption of chlorophyll in the red light band and the multiple scattering in the mesophyll cell structure and canopy in the near-infrared band, they are often used for multiple combinations such as ratio, difference, and linear combination, forming a clear contrast to enhance or reveal the hidden plant information. However, despite the extensive research performed on crops such as wheat (*Triticum aestivum* L.), studies on the remote sensing monitoring of the vertical distribution of chlorophyll content in maize is lacking, perhaps due to the difficulties of this application [4–9]. Soil and plant analyzer development (SPAD) is one of the most important indicators for the characterization of plant chlorophyll relative content. SPAD measurements are fast and can reflect the characteristics of the plant chlorophyll content, and are thus often used in crop health status evaluations and plant physiological research (e.g., with rice, vegetables, fruits) [1,10–14]. Chlorophyll absorption peaks appear in the blue region (400–500 nm) and red region (600–700 nm), but not in the near-infrared region. Using this absorption property of chlorophyll, SPAD measures the absorption rate of leaves in the red region and near-infrared region through the absorption rate of these two parts of the region, to calculate a SPAD value. Compared with other methods for measuring the amount of chlorophyll in plants such as rice, including chlorophyll measurement, infrared digital camera analysis, and so on, SPAD is portable and enables quick, simple, and nondestructive measurement. It is of great significance to obtain SPAD values of leaves at different vertical positions of maize canopy by remote sensing.

The monitoring of the vertical distribution of maize (*Zea mays* L.) canopy components via remote sensing approaches proves to be a difficult task. First, the vertical height of maize is higher than that of wheat. The upper region of the crop canopy typically obtains a sufficient amount of light, thus developing the upper leaves more than those in the lower region. This consequently results in the shading of the lower leaves by the upper leaves to a greater extent than that of wheat. Vertical observations via remote sensing is thus limited in maize canopies. In general, 6 to 8 leaves from the top of the canopy can be detected [15]. Moreover, compared with maize, wheat plants have a lower size and are densely planted, allowing for accurate observations of wheat fields at the canopy scale. By contrast, there is a great heterogeneity in the horizontal direction within maize crops, with a big difference between observations on and between ridges. This heterogeneity decreases with the continuous increase in the observation scale. Furthermore, the maize plant structure varies greatly with the growth period, and thus, there is a large difference between the vegetative and reproductive growth stage. The ridge does not begin to close until the tasseling stage, and thus, the soil background affects the response of the spectrum acquired by the canopy [16–18]. In-depth hierarchical spectrum analysis has previously been employed with the crop vertical canopy spectrum matching method to determine crop middle- and lower-layer nitrogen levels and chlorophyll content, with results revealing the leaf area to be vertically distributed in a bell shape [19,20] and chlorophyll content [21]. In addition, the vertical distribution of leaf area index (LAI) and chlorophyll content in the maize canopy has been observed to vary with the growth stage [21]. In the growth and reproductive development stages (i.e., maize early and late growth periods), the vegetation coverage and sheltering of the male ear will affect the selection and accuracy of the optimal monitoring method for the vertical distribution of canopy chlorophyll content.

The light absorption capacity of the upper layer is stronger than that of the lower layer in maize canopy. The vertical spectrum of maize is able to detect 7–9 leaves from the top of

the canopy, yet the multi-angular spectrum of the canopy can obtain a vertical distribution of the chlorophyll content. However, the monitoring ability of the multi-angular approach for the pre- and post-growth periods remains unclear. In particular, two key issues are of interest: (1) To determine if the optimal observation method for chlorophyll content of each vertical layer is consistent between the vegetative and reproductive growth stages of maize; and (2) to evaluate the detection ability of the optimal observation method for the chlorophyll content of different layers of maize across the growth period.

In the current paper, we integrate canopy-scale spectral data under different view zenith angles (VZAs) with an agronomic-based spatiotemporal distribution model of leaf SPAD values to determine the maximum detection depth of chlorophyll in maize canopy leaves. We then investigate the optimal spectral combination and spectral index for the SPAD values of maize leaves at various layers to establish the optimal observation model for the target layer SPAD value monitoring.

2. Materials and Methods

2.1. Experimental Site and Design

(1) Experimental site 1

Field experiments were conducted in 2017 at the Xiaotangshan Precision Agriculture Experimental Base (40°110N, 116°270E) in Beijing City, China. The cropping system is a winter wheat (*Triticum aestivum* L.) summer maize rotation, which is the most commonly used approach in North China. The field site is located in a warm temperate climate zone in a semi-moist continental monsoon region. The annual average temperature, precipitation, and sunlight hours are 10–12 °C, 600–700 mm, and 2700–2800 h, respectively. The seasonal distribution of precipitation is uneven, with 70% of the precipitation occurring from July to September. The climatic characteristics are suitable for many field crops, including wheat, maize, and soybeans (*Glycine max* L.), all of which can only be harvested twice a year. It should be noted that during the growing period of maize, the main growth stages are: Emergence stage (VE), First-Leaf stage (V1), Second-Leaf stage (V2), Fourth-Leaf stage (V4), Sixth-Leaf stage (V6), Tenth-Leaf stage (V10), Fourteen-Leaf stage (V14), Tassel stage (VT), Silking stage (R1), Blister stage (R2), Milk stage (R3), Dough stage (R4), Dent stage (R5), Maturity stage (R6). Measurements were taken on June 27 (sixth-leaf stage, V6), July 12 (tenth-leaf stage, V10), July 30 (tassel stage, VT), and August 21 (milk stage, R3) in 2017.

The experiment consisted of three plant geometry treatments with 15 varieties, including five horizontal (Nongda 80, 96–3, Zhengdan 958, Yuyu 22, and Nongda 108), five intermediate (Jingyu 7, Zhongyuandan 32, Zhongdan 9409, Gaoyou 115, and Zhongnuo 2), and five upright (Tangyu 10, Hudan 2000, Jingshibai 1, Tangkang 5, and Jiangzao 13) varieties. The plot size and planting distance of all treatments were 15 m × 7 m and 70 cm × 30 cm, respectively. All treatments were conducted under the same management practices according to the local standards for summer maize production.

(2) Experimental site 2

Field experiments were conducted in 2004 at the Beijing Academy of Agriculture and Forestry Sciences Experimental Base (39°58'N, 116°20'E) in Beijing City, China. The natural environment is similar to site 1 (average temperature, soil precipitation, and sunlight hours, etc.), while the experimental design is distinct. Measurements were performed on June 4 (sixth-leaf stage, V6), June 13 (tenth-leaf stage, V10), June 25 (tassel stage, VT), July 19 (silking stage, R1), August 8 (milk stage, R3), and September 13 (dent stage, R5) in 2004.

The experiment involved three plant geometry treatments with 3 varieties, including horizontal (Nongdagaoyou115), intermediate (Nongda108), and upright (Zhengdan958) varieties. The plot size and planting distances of the treatments were 11 m × 10 m and 60 cm × 30 cm, respectively. All treatments were conducted under the same management practices according to the local standards for summer maize production.

(3) Experimental site 3

The experiment was carried out during the 2018 summer maize growth period in Dajianchang Town ($39^{\circ}54.2'N$, $117^{\circ}26.9'E$), Wuqing District, Tianjin City, China. The principal crops in the farmland region are winter wheat and summer maize in rotation. The area is flat and the cultivated land is distributed in patches, which is convenient for experimental applications. The experimental area is located 126 km away from site 1 and, thus, the environment is similar to site 1 (average temperature, soil precipitation, and sunlight hours). As each family plants their fields at different times, the growth stage of maize crops is heterogeneous, favoring scientific research. Measurements were made on July 5 (sixth-leaf stage, V6), August 3 (tenth-leaf stage, V10), August 17 (tassel stage, VT), and September 5 (milk stage, R3) in 2018. The principle maize varieties were Jiyan 118, Jiyan168, and Shiyu 9.

2.2. Multi-Angular Spectral Reflectance Measurements

The multi-angular frame is a device equipped with a spectrometer for multi-angular measurements (Figure 1). The frame core realizes the multi-angular observation at the specified angle. When the VZA is changed, the pointing target of the spectrometer cannot be changed. In order to adapt to features of different heights, the center point of the angle rotation can be adjusted. Furthermore, the distance between the sensor observation position and the target is adjusted when the field of view size of the target is changed. The multi-angular frame uses a manual rotating drive to maneuver an inclined support rod in order to adjust the detection field of view angle, where the angle varies from 0° to 60° , with an incremental step of 10° . The angle corresponds to the backscattering direction (measured back to the sun). The adjustment is performed by moving a 4-section adjustment carbon fiber tube, and the observation sensor measures the distance to the target. The adjustment range is from 0.9 to 3.5 m, and the sensor can be fine-tuned in the horizontal position within an 8 cm range.



Figure 1. Multi-angular spectral reflectance acquisition in sixth-leaf stage.

The canopy spectral reflectance was measured using an ASD FieldSpec[®] Pro FR spectroradiometer (Analytical Spectral Devices, Boulder, CO, USA) between 10:00 AM and 2:00 PM (Beijing local time) under clear sky conditions. The ASD was configured with a spectral range from 350 to 2500 nm, a 1.4 nm sampling interval between 350 and

1000 nm, a 2 nm sampling interval between 1000 and 2500 nm, and a field of 25°. The instrument has a spectral resolution of 3 nm at 700 nm, and a 10 nm spectral resolution at 1400 and 2100 nm. The spectral data were subdivided into 1 nm bandwidths using a self-driven interpolation method of the ASD and saved to the connected PC. We used data from the spectral region of 350–1050 nm, which is commonly used for the spectral analysis of vegetation. A fiber-optic probe was fixed at the top end of a height-adjustable inverted-L pole. All canopy reflectance measurements were obtained from a distance of 1.6 m above the maize canopy. The reflectance measurements were collected randomly at three sites in each plot and subsequently averaged to represent the canopy reflectance of the plot.

2.3. Leaf Stratification and SPAD Measurements

The majority of previous research on maize crops employ agricultural-based stratification methods. For example, functional leaves are considered as the second layer of the vertical distribution, and the region above the functional leaves is taken as the first layer. However, the location of different layers changes with the growth period, which consequently affects the remote sensing-derived inversions and reduces the robustness of the inversion model. In this paper, based on existing research using canopy vertical spectroscopy [18,22], the maize was divided into vertical canopy layers according to the height from the canopy, namely, the canopy depth. The 1st–4th leaves from the top of the canopy were used as the 1st layer; the 5th–8th leaves were used as the 2nd layer; the 9th–12th leaves were used as the 3rd layer; and the 13th+ leaves as the 4th layer. If the number of leaves in the sample data at a certain growth period does not meet the layer requirements, the sample takes a component of the vertical layer. The average number of leaves in the V6 growth period was 7, with some samples containing only the 1st and 2nd layers, while the average number of leaves in the V10 growth period was 12, with some samples lacking the 4th layer.

The measurement process can be described as follows: (1) The leaves at the target position with no disease, physiological spots, and mechanical damage were selected; (2) a soft brush was used to remove the sand and dust on the leaf surface; and (3) the measurements (SPAD value, LAI, etc.) of 3 leaf components were averaged and taken as the final value.

The total amounts of chlorophyll content in each leaf (SPAD value) and vertical layer were calculated following Ciganda et al. [21], while the area of each leaf was measured via the length width method:

$$S_{leaf} = Length_{leaf} * Width_{leaf} * 0.73 \quad (1)$$

$$S_{layer} = \sum_{i=1}^n S_{leaf} \quad (2)$$

$$SPAD_{layer} = \sum_{i=1}^n SPAD_{leaf} * S_{leaf} / S_{layer} \quad (3)$$

where S_{leaf} denotes a single leaf area; S_{layer} is the leaf area of a layer; $SPAD_{layer}$ is the SPAD value of the layer; $SPAD_{leaf}$ is the SPAD value of the leaf; $Length_{leaf}$ and $Width_{leaf}$ represent the leaf length and leaf width, respectively; and S_{leaf} is the SPAD value of a single leaf.

2.4. Vegetation Indices and Data Analysis

Numerous multi-channel spectral indices have been developed to detect ecological functional parameters (e.g., vegetation biophysical and biochemical parameters) and have been successfully applied to chlorophyll content estimations [22]. We employ the indices from the previous literature in the current paper (Table 1).

Table 1. Spectral vegetation indices employed in this paper.

Short Name	Name	Formula	Applications	Reference
PSSRa	Pigment specific simple ratio	R_{800}/R_{680}	Vegetation; Chlorophyll	[23]
PSSRb	Pigment specific simple ratio	R_{800}/R_{635}	Vegetation; Chlorophyll	[23]
RR710	Red edge reflectance ratio	R_{750}/R_{710}	Vegetation; Chlorophyll	[24]
RR720	Red edge reflectance ratio	R_{740}/R_{720}	Vegetation; Chlorophyll	[25]
PSNDA	Pigment specific normalized difference	$(R_{800} - R_{680})/(R_{800} + R_{680})$	Chlorophyll; LAI; PAR; Crop yield; et al.	[23]
PSNDb	Pigment specific normalized difference	$(R_{800} - R_{635})/(R_{800} + R_{635})$	Vegetation; Chlorophyll	[23]
NDVI	Normalized difference vegetation index	$(R_{800} - R_{670})/(R_{800} + R_{670})$	Chlorophyll; LAI; Crop yield; et al.	[26]
ND705	Normalized difference red edge	$(R_{750} - R_{705})/(R_{750} + R_{705})$	Vegetation; Chlorophyll	[26]
PRI	Photochemical reflectance index	$(R_{531} - R_{570})/(R_{750} + R_{705})$	Vegetation; Chlorophyll	[27]
CIred edge	Chlorophyll index red edge	$(R_{750}^{-1} - R_{700}^{-1})/R_{700}$	Vegetation; Chlorophyll	[28]
CIgreen	Chlorophyll index green	$(R_{750}^{-1} - R_{550}^{-1})/R_{550}$	Vegetation; Chlorophyll	[28]
SIPI	Structure insensitive pigment index	$(R_{800} - R_{445})/(R_{800} - R_{680})$	Vegetation; Chlorophyll	[29]
EPI	Eucalyptus pigment index	$(R_{850} - R_{710})/(R_{850} - R_{680})$	Vegetation; Chlorophyll	[30]
mSR705	Modified simple ratio	$(R_{750} - R_{445})/(R_{705} - R_{445})$	Vegetation; Chlorophyll	[31]
MTCI	MERIS terrestrial chlorophyll index	$(R_{750} - R_{710})/(R_{710} - R_{680})$	Chlorophyll	[32]
REIP	Red edge inflection point	$R_{700} + 40[(R_{670} + R_{780})/2 - R_{700}]/(R_{740} - R_{700})$	Vegetation; Chlorophyll; Red-edge position	[25]
MCARI	Modified CARI	$[(R_{700} - R_{670}) - 0.2(R_{700} - R_{550})] * (R_{700}/R_{670})$	Vegetation; Chlorophyll	[33]
TCARI	Transformed CARI	$3[(R_{700} - R_{670}) - 0.2(R_{700} - R_{550}) * (R_{700}/R_{670})]$	Chlorophyll	[34]
OSAVI	Optimized SAVI	$(1 + 0.16) * (R_{800} - R_{680}) / (R_{800} + R_{680} + 0.16)$	Vegetation; Soil	[35]
MCARI/OSAVI	MCARI/OSAVI	MCARI/OSAVI	-	-
TCARI/OSAVI	TCARI/OSAVI	TCARI/OSAVI	-	-

Altogether, 55 maize samples were collected in 2004, 2017, and 2018. As our data included different growth stages of maize among the three years, samples in each growth stage in each year were randomly divided into two datasets: Two thirds as the training dataset and one third as the validation dataset. In addition, 24 samples were used to build estimation models and validate SPAD value prediction for the early growth stage. Further, 31 samples were used for calibration and validation for the late growth stage. Analyses were performed using MATLAB 9.0 (The MathWorks, Inc., Natick, MA, USA) and Excel 2013 (The Microsoft Corporation, Inc., Redmond, WA, USA). The performance of the model was estimated by comparing the differences in prediction abilities using the coefficient of determination (R^2), root-mean-square error (RMSE), and magnitude of relative error (MRE%). High R^2 and low RMSE and MRE values denote high model precision for SPAD value predictions.

3. Results

3.1. Temporal and Spatial Distribution of Chlorophyll Content

The vertical distribution of the chlorophyll content at different vertical leaf positions initially increased and subsequently decreased with the canopy depth (i.e., the distance from the top of the canopy). This is in agreement with the majority of crops [15]. The leaves at the top of the canopy were typically less developed, with an increasing accumulation of chlorophyll content; thus, the chlorophyll content was less than that of the functional leaves at the center of the canopy. Due to shading by the upper leaves, the leaves below the functional leaves demonstrated a decrease in photosynthesis levels with the increasing vertical layer. This also reduced the chlorophyll content. In addition, as the growth period continued, the chlorophyll content of the canopy changed with the vertical position, becoming more heterogeneous (Figure 2). More specifically, the chlorophyll content of the functional leaves was observed to increase, while the chlorophyll content of nonfunctional leaves declined.

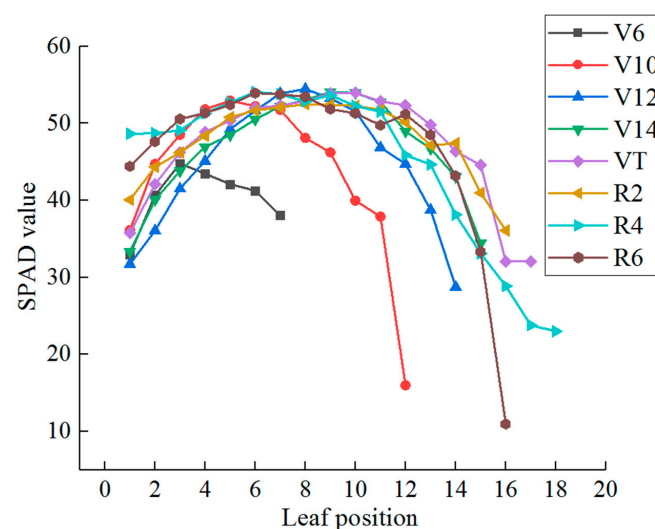


Figure 2. Vertical leaf position soil and plant analyzer development (SPAD) values at different growth stages.

The maize canopy leaves at different growth stages were stratified according to the distance from the canopy. The vertical distribution of the chlorophyll content at the 1st, 2nd, 3rd, and 4th layers was in agreement with that of the leaf position (Table 2), initially increasing and then decreasing with canopy depth. The chlorophyll contents of the 2nd and 3rd layers was higher than those of the 1st and 4th layers. The 1st, 2nd, and 3rd layers generally exhibited a gradual increasing law with the growth period, while the chlorophyll content of the 4th layer initially increased and then decreased. The heterogeneity of the SPAD values at the 3rd layer of the early growth stage was higher than those at the 1st and

2nd layers, while that of the 4th layer of the late growth stage was higher than those of the other layers (8.38% and 14.52%, respectively). The heterogeneity of SPAD values in the upper layer at the later stage of the growth period was also higher (11.36%). This might be attributed to the uneven development of the upper leaves due to the slower growth rate at this stage. Moreover, the male panicle shielding at the late growth stage increased the difficulty of SPAD measurements on the 1st blade layer.

Table 2. Descriptive statistics of SPAD values across vertical canopy layers and maize growth stages.

Layer	<i>n</i>	Max	Min	Mean	SD ⁺	CV ⁺⁺ (%)
Early growth stage						
1st-layer	24	57.30	45.30	51.97	3.78	7.27
2nd-layer	24	65.90	50.10	61.34	4.45	7.25
3rd-layer	24	65.50	48.10	59.90	5.02	8.38
Late growth stage						
1st-layer	31	62.10	38.20	51.65	5.87	11.36
2nd-layer	31	66.40	46.60	61.44	5.22	8.50
3rd-layer	31	67.50	44.20	61.21	5.97	9.75
4th-layer	31	65.80	36.50	56.57	8.21	14.52
All stages						
1st-layer	55	62.10	38.20	51.79	5.02	9.70
2nd-layer	55	66.40	46.60	61.40	4.86	7.91
3rd-layer	55	67.50	44.20	60.64	5.56	9.17
4th-layer	31	65.80	36.50	56.57	8.21	14.52

⁺ Standard deviation. ⁺⁺ Coefficient of variation.

The correlation between layers was observed to decrease with the distance between layers (Table 3), with coefficients of determination of 0.47, 0.94, and 0.85 between the 1st and 2nd layers, the 2nd and 3rd layers, and the 3rd and 4th layers, respectively. In addition, the coefficients of determination between the leaf chlorophyll content of the 1st layer and the 3rd and 4th layers were 0.32 and 0.12, respectively. The relationship between the chlorophyll content of the 1st layer and the other layers was relatively weak. This might be attributed to the new leaves in the upper region, as the chlorophyll content changes greatly when the growth and development are completely transformed into the lower leaves. This could explain the significant difference of the chlorophyll content information between the 1st layer and the 2nd and lower layers and demonstrates the ability of our approach to monitor the chlorophyll content of the lower leaves shaded by the upper leaves.

Table 3. Correlation of SPAD values among different vertical layers (R^2).

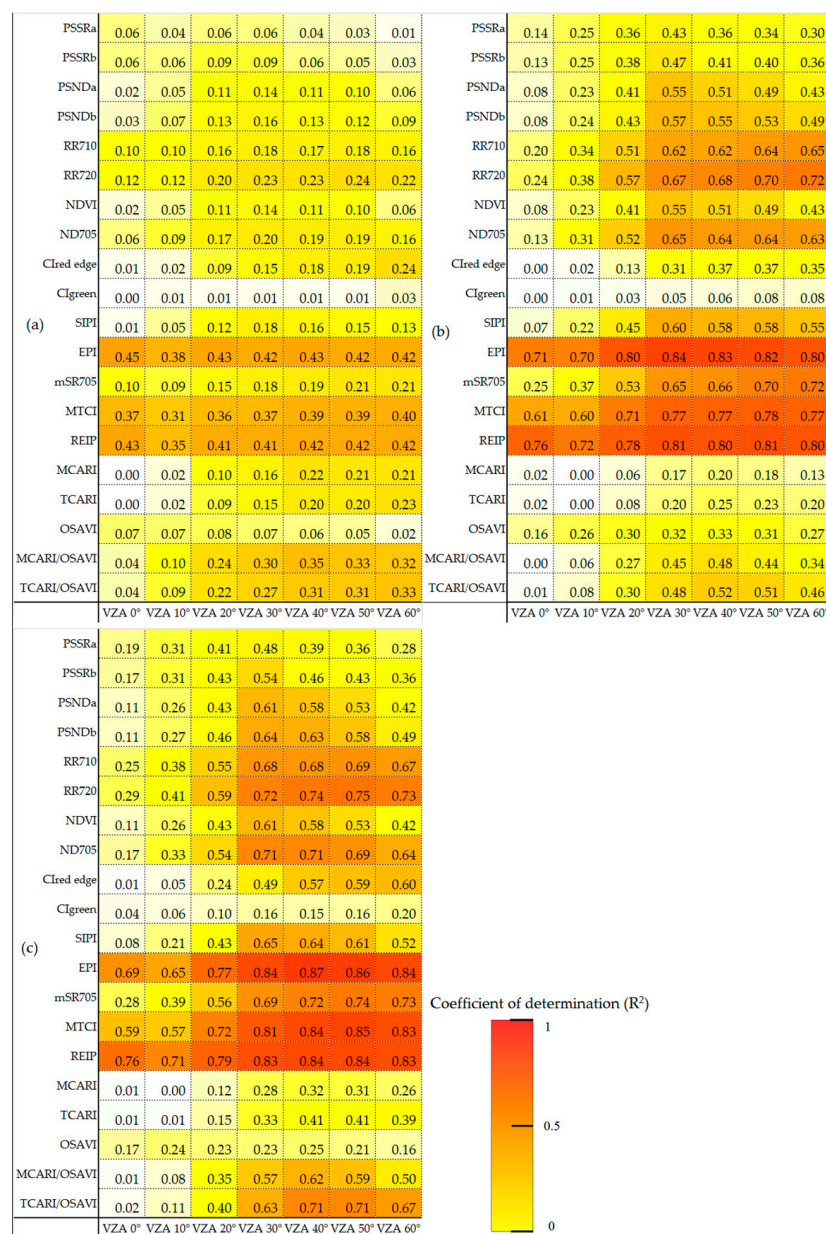
Layer	1st-Layer	2nd-Layer	3rd-Layer	4th-Layer
1st-layer	1	-	-	-
2nd-layer	0.47	1	-	-
3rd-layer	0.32	0.94 *	1	-
4th-layer	0.12	0.66	0.85 *	1

Analyses were performed using Pearson's correlation. * Significant at 0.01 level based on a two-tailed test.

3.2. Correlation Analysis of SPAD Value at Different Vertical Layers and Chlorophyll Sensitivity Indices

Figures 3 and 4 show the coefficients of determination between different chlorophyll sensitivity indices at the early and late growth stages and SPAD values at different vertical layers, from which the eucalyptus pigment index (EPI) and red edge inflection point (REIP) index were selected. Among the chlorophyll sensitivity indices adopted in this study, the EPI and REIP indices exhibited the best performance during the early and late growth stages, achieving the strongest correlations with SPAD values at all layers. Thus, we selected

these two indices for further analysis. Figure 5 presents the correlation analysis between the chlorophyll content and the EPI and REIP indices under different layers and VZAs, respectively. The coefficients of determination of the upper canopy chlorophyll increased with observations, while those of the lower canopy initially increased and subsequently decreased. More specifically, the coefficients of determination between the EPI and the upper three layers increased with the VZA, while the 4th-layer coefficients of determination were initially stronger and then weakened. For the case of the REIP index, the 1st and 2nd layers increased with the VZA, while the 3rd and 4th layers initially increased and subsequently decreased.



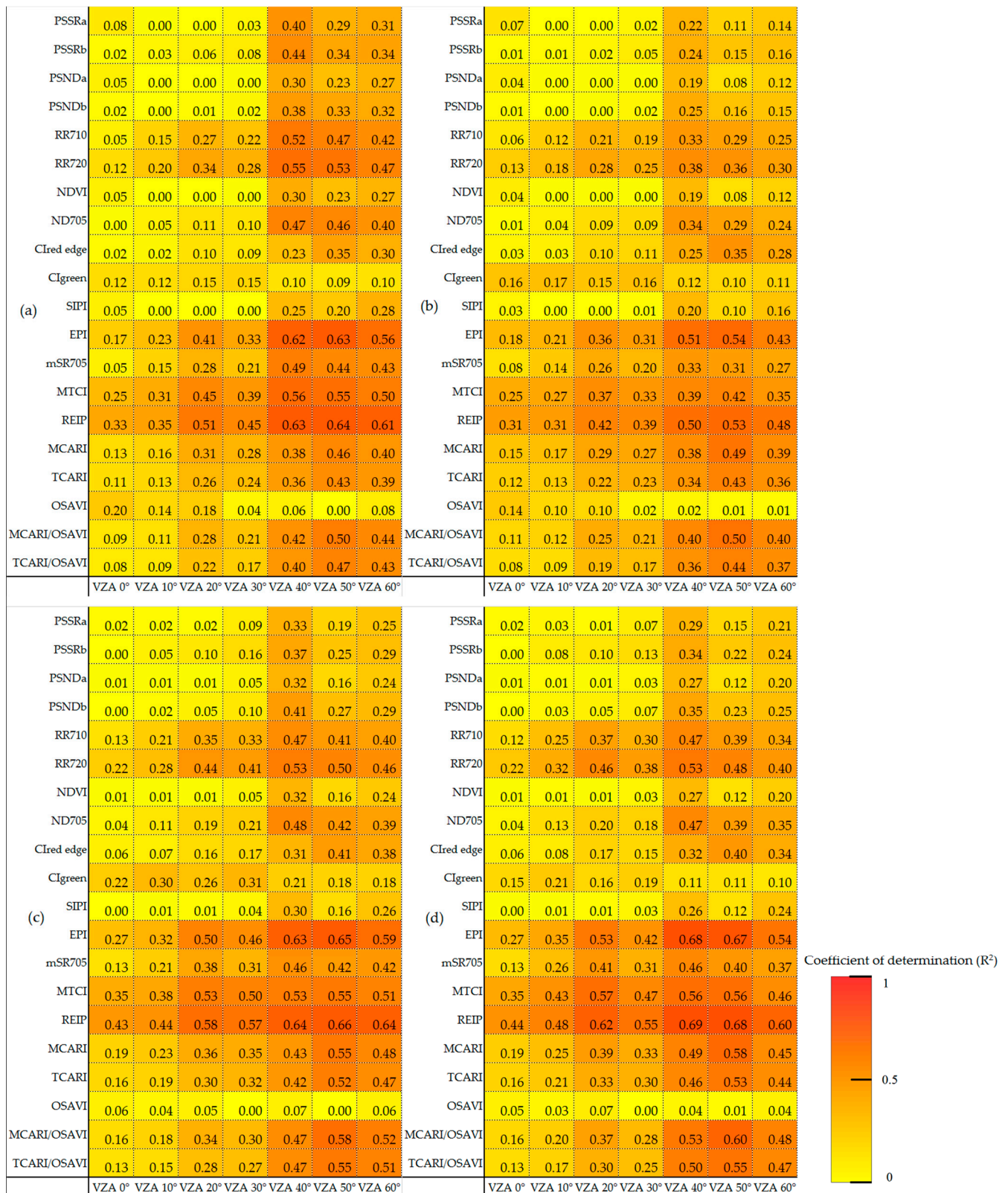


Figure 4. Coefficients of determination between the SPAD value in the late growth stage and the chlorophyll sensitivity index of different VZAs: (a) 1st layer, (b) 2nd layer, (c) 3rd layer, and (d) 4th layer.

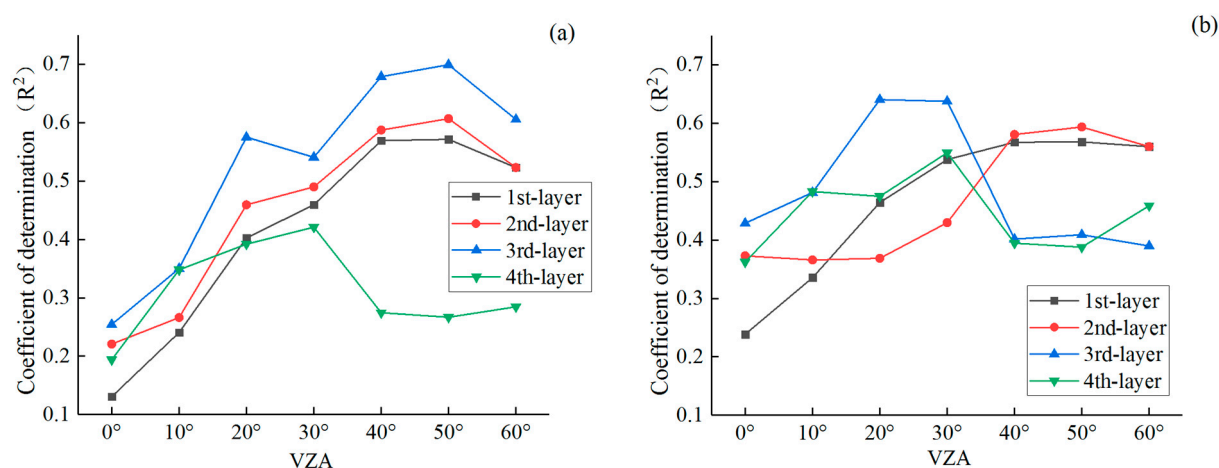


Figure 5. Coefficients of determination between SPAD values and indices under different layers and VZAs: (a) Eucalyptus pigment index (EPI) and (b) red edge inflection point (REIP) index.

3.3. Optimized Monitoring VZAs for Vertical Leaf SPAD Estimations

Table 4 reports the optimal VZA per layer, based on the correlation trend of chlorophyll content at different layers with different VZAs. During the early growth stage of maize, the VZA increased with observation depth. Based on the EPI and REIP indices, we adopted the VZAs 0°, 30°, and 50° to monitor the chlorophyll content of the 1st-, 2nd-, and 3rd-layer stages of the early growth period, while for the late growth period, the VZA of 50° was used for the 1st, 2nd, and 3rd layers. For a specific depth, the VZAs 40° and 50° were used to continue the chlorophyll content observations. Figures 6–9 present the relationship between the chlorophyll content and the indices under the selected VZAs.

Table 4. Optimal selection of monitoring VZAs for different target layers.

Layer	Early Growth Stage		Late Growth Stage	
	EPI	REIP	EPI	REIP
1st-layer	VZA 0°	VZA 0°	VZA 50°	VZA 50°
2nd-layer	VZA 30°	VZA 30°	VZA 50°	VZA 50°
3rd-layer	VZA 40°	VZA 40°	VZA 50°	VZA 50°
4th-layer	—	—	VZA 40°	VZA 40°

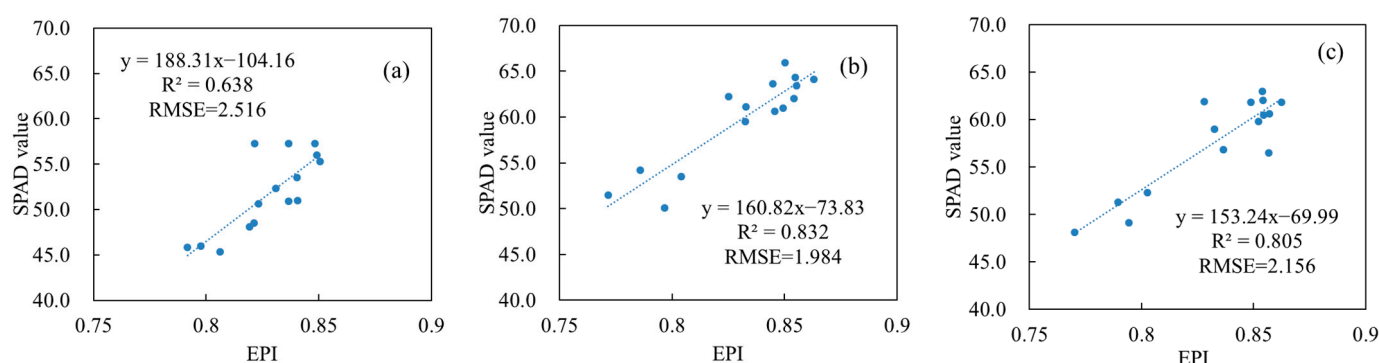


Figure 6. Relationship between SPAD values at different layers and the EPI under the optimum VZA in the early growth stage: (a) 1st layer, (b) 2nd layer, and (c) 3rd layer.

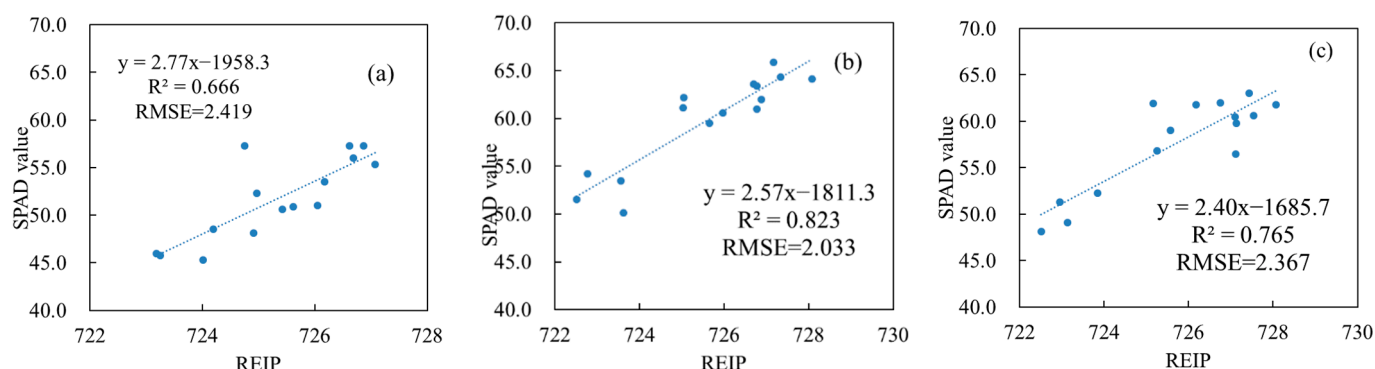


Figure 7. Relationship between SPAD values at different layers and the REIP index under the optimum VZA in the early growth stage: (a) 1st layer, (b) 2nd layer, and (c) 3rd layer.

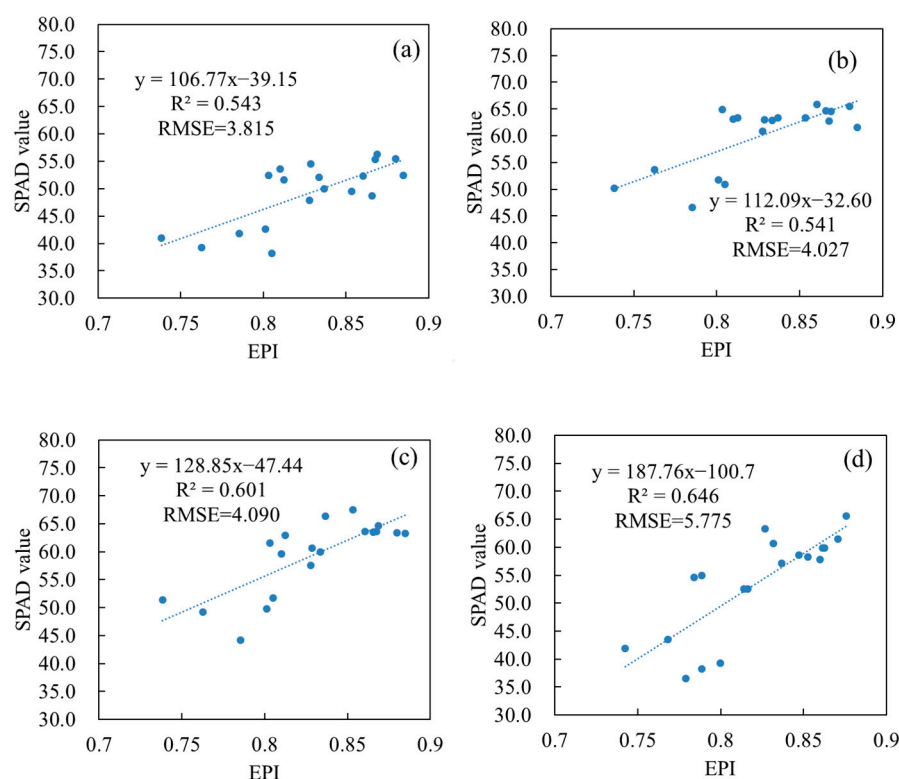


Figure 8. Relationship between SPAD values at different layers and the EPI under the optimum VZA in the late growth stage: (a) 1st layer, (b) 2nd layer, (c) 3rd layer, and (d) 4th layer.

3.4. Verification of Vertical Leaf SPAD Estimation Models

Table 5 evaluates the accuracy of the chlorophyll content determined from our proposed approach under the different monitoring layers, using the monitoring results of EPI and REIP indices in Table 5. The monitoring accuracy of both indices at the 2nd and 3rd layers surpassed that of the 1st layer in the early and late growth stages. In particular, the RMSE of the EPI and REIP monitoring results reached 4.14 and 4.61 in the early and late stages, respectively. Although the late growth stage RMSE was not large, the R^2 value between the predicted and true data was small. This might be attributed to the incomplete leaf growth in the early stage of maize, with the upper layer of the leaves at the top of the canopy having a smaller area than those of the 2nd and 3rd layers. The information contained in the canopy spectrum of the 1st layer was less than those of the other layers. Moreover, the 2nd- and 3rd-layer leaf SPAD values were determined as more suitable than that the 4th layer for the monitoring of the early and late growth stages. More specifically, the 4th layer of leaves appeared in the late growth period. The EPI and REIP monitoring

results were worst among the four layers. The RMSE values reached 4.80 and 7.85, respectively, indicating the monitoring ability of the 4th layer to be incomparable with those of the other canopy layers.

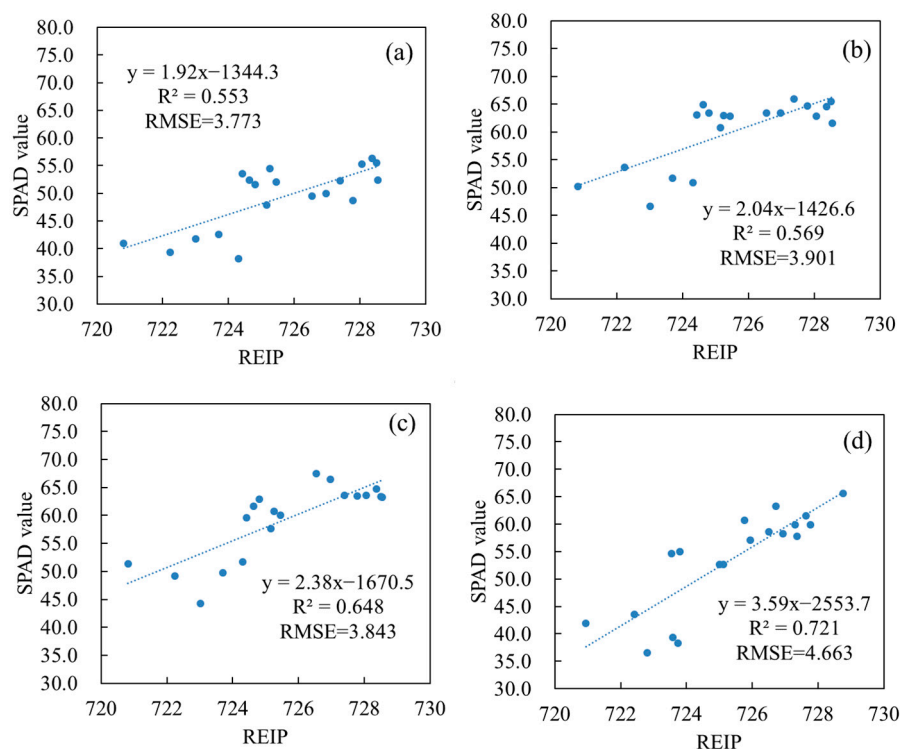


Figure 9. Relationship between SPAD values of different layers and the REIP index under the optimal VZA in the late growth stage: (a) 1st layer, (b) 2nd layer, (c) 3rd layer, and (d) 4th layer.

Table 5. Accuracy evaluation results.

Layer	EPI			REIP		
	R^2	RMSE	MRE (%)	R^2	RMSE	MRE (%)
Early growth stage						
1st-layer	0.32	4.14	6.90	0.34	4.61	7.96
2nd-layer	0.33	1.71	2.25	0.12	2.31	3.13
3rd-layer	0.71	1.11	1.45	0.57	1.00	1.27
Late growth stage						
1st-layer	0.22	2.97	4.28	0.28	3.16	5.22
2nd-layer	0.62	3.50	5.07	0.62	5.02	7.46
3rd-layer	0.57	2.80	3.57	0.63	4.55	6.41
4th-layer	0.49	4.80	6.78	0.38	7.85	11.47

4. Discussion

Although the vertical distribution of crop components has been demonstrated in numerous studies [36–39], the accuracy of remote sensing monitoring approaches has much room for improvement. The stratification method employed in this paper overcomes the limitations of those in the previous literature, for example, variations in the stratification vertical depth position with growth stage and inconsistent canopy depth standards. Thus, the proposed approach improves on the detection of depth via remote sensing and is more suitable for research on remote sensing monitoring methods.

Previous work adopted complex indices, like TCARI and MCARI indices (Table 1), for the estimation of chlorophyll content for the wheat canopy [33,34]. However, in the current paper, EPI and REIP are proved to be more effective. This may be due to the higher

vegetation coverage of maize compared to wheat, such that the surface soil contributes less to the spectrum, and thus, the soil background has less of an influence on the spectrum. In addition to the EPI and REIP indices, the RR710, RR720, ND705, SIPI, mSR705, and MTCI indices (Table 1) also have better chlorophyll sensitivity responses than other indices. Most of these indices include the spectral response bands around 700–720 nm. It is guessed that the above bands can take into account both the electromagnetic wave penetration of the infrared band and the chlorophyll sensitivity response. In addition, it is very likely that the band settings of the EPI and REIP indices conform to the measurement principle of the SPAD measuring instrument, resulting in a better sensitivity of these two indices [33,40].

This paper determines the optimal observation method by maximizing the coefficient of determination between the indices at different VZAs and the SPAD values at the vertical layers of the maize canopy leaves. The selected VZAs are not consistent across growth periods. The VZAs 0°, 30°, and 40° are selected for the 1st, 2nd, and 3rd layers of the early growth period, while during the later stages, 50° is used. As the selections are based on the EPI and REIP indices, the differences among growth periods are independent of spectral features and can rather be attributed to the following factors. First, tassels do not grow on the top of the plant in the early stage; thus, the spectrometer avoids the shading of the tassels and directly receives the signal of the leaf spectrum. However, during the later period, tassels are present on the top of the maize canopy, particularly for small-angle observations. The tassels act as obstacles for the spectral signal of the leaves below them [7,41,42], and spectral information of the tassels is distinct to that of the leaves. In addition, the plant structure of maize varies across the growing season. The plant takes an umbrella-like form during the early stage, and the leaf size gradually decreases from the top of the canopy to the bottom, while at the later stages, the plant exhibits a spinning cone-like shape, and the size of the blade initially increases and then decreases from the top of the canopy to the bottom. The functional leaf has the largest blade size. Furthermore, at the early growth stage, the maize is not fully developed, the plant size is small, and the growth is sparse and unsealed. The spectrum of the leaves in the lower canopy can reach the sensor without being shaded by other plants. By contrast, in the late growth period, the lower leaves of the canopy are shaded by the tassels and upper leaves, and oblique observations will be shaded by other plants [43–47]. Thus, the detection ability of the canopy tilt observation spectrum is largely affected by the leaf tilt structure parameters of the maize plant. Further discussions relating to this are reserved for future studies.

Due to limited resources and space, this paper has several limitations. For example, the maize varieties and planting methods followed the northern China standards [48,49]. There may be some differences in the results of other maize varieties and planting methods in other regions. Although the vertical stratification method of the canopy in this paper is more suitable for remote sensing-based vertical distribution monitoring compared to previous methods, the stratification can greatly simplify the research object of the vertical distribution elements and simplify the problem. However, following artificial stratification, the vertical variation in chlorophyll content may be weakened to a certain extent, and information may be lost. In addition, the current paper did not explore the optimal index form of maize chlorophyll vertical distribution monitoring based on multi-angular monitoring [33,40]. This will be investigated in future work. Finally, this work does not focus on optimizing the spectral bands and band combinations for the chlorophyll content of different vertical layers. Rather, we focus on improving the monitoring accuracy of the chlorophyll content at a specific level. Future research can employ our results to extend this work.

5. Conclusions

Based on canopy-scale multi-angular spectroscopy, this paper explored the maximum detection depth of maize canopy chlorophyll content (SPAD value) and determined the optimal VZA and monitoring model for different layers of SPAD values and spectrally detectable depths. The results demonstrate the ability of the proposed stratification method

to effectively stratify the canopy leaves from the bottom to the top of the canopy. Based on the correlation between the selected EPI and REIP indices and the chlorophyll content, we selected the VZAs of 0°, 30°, and 40° to monitor the chlorophyll content of the 1st, 2nd and 3rd layers, respectively, and 50° for the middle and late stages. The results demonstrate the ability of canopy multi-angular spectral reflectance to accurately estimate the maize canopy chlorophyll content vertical distribution, with the VZAs of different vertical layers varying between the early and late growth stages.

Author Contributions: B.W. performed the data analysis and wrote the manuscript. W.H. and H.Y. guided the study and discussed the methods and results. P.L., H.W. and W.K. provided suggestions for the study, and reviewed and edited the manuscript. B.W., H.Y., P.L. and Y.R. conducted the field experiments. All authors have read and agreed to the published version of the manuscript.

Funding: This research was funded by the National Natural Science Foundation of China (41871339, 41901369), Future Star Talent Program of Aerospace Information Research Institute, Chinese Academy of Sciences (Huichun Ye), and National Special Support Program for High-level Personnel Recruitment (Wenjiang Huang).

Acknowledgments: We gratefully acknowledge the Xiaotangshan Precision Agriculture Experimental Base for the experiments support.

Conflicts of Interest: The authors declare no conflict of interest.

References

1. Zhao, B.; Ata-Ul-Karim, S.T.; Liu, Z.; Zhang, J.; Xiao, J.; Liu, Z.; Qin, A.; Ning, D.; Yang, Q.; Zhang, Y. Simple assessment of nitrogen nutrition index in summer maize by using chlorophyll meter readings. *Front. Plant Sci.* **2018**, *9*, 11. [\[CrossRef\]](#)
2. Hirose, T.; Werger, M.J. Nitrogen use efficiency in instantaneous and daily photosynthesis of leaves in the canopy of a *Solidago altissima* stand. *Physiol. Plant.* **1987**, *70*, 215–222. [\[CrossRef\]](#)
3. Dreccer, M.; Van Oijen, M.; Schapendonk, A.; Pot, C.; Rabbinge, R. Dynamics of vertical leaf nitrogen distribution in a vegetative wheat canopy. Impact on canopy photosynthesis. *Ann. Bot.* **2000**, *86*, 821–831. [\[CrossRef\]](#)
4. He, J.; Zhang, X.; Guo, W.; Pan, Y.; Yao, X.; Cheng, T.; Zhu, Y.; Cao, W.; Tian, Y. Estimation of vertical leaf nitrogen distribution within a rice canopy based on hyperspectral data. *Front. Plant Sci.* **2019**, *10*, 1802. [\[CrossRef\]](#)
5. Luo, J.; Ma, R.; Feng, H.; Li, X. Estimating the total nitrogen concentration of reed canopy with hyperspectral measurements considering a non-uniform vertical nitrogen distribution. *Remote Sens.* **2016**, *8*, 789. [\[CrossRef\]](#)
6. Duan, D.; Zhao, C.; Li, Z.; Yang, G.; Yang, W. Estimating total leaf nitrogen concentration in winter wheat by canopy hyperspectral data and nitrogen vertical distribution. *J. Integr. Agric.* **2019**, *18*, 1562–1570. [\[CrossRef\]](#)
7. Li, L.; Jákli, B.; Lu, P.; Ren, T.; Ming, J.; Liu, S.; Wang, S.; Lu, J. Assessing leaf nitrogen concentration of winter oilseed rape with canopy hyperspectral technique considering a non-uniform vertical nitrogen distribution. *Ind. Crop. Prod.* **2018**, *116*, 1–14. [\[CrossRef\]](#)
8. Hirooka, Y.; Homma, K.; Shiraiwa, T. Parameterization of the vertical distribution of leaf area index (LAI) in rice (*Oryza sativa* L.) using a plant canopy analyzer. *Sci. Rep.* **2018**, *8*, 1–9. [\[CrossRef\]](#)
9. Ye, H.; Huang, W.; Huang, S.; Wu, B.; Dong, Y.; Cui, B. Remote estimation of nitrogen vertical distribution by consideration of maize geometry characteristics. *Remote Sens.* **2018**, *10*, 1995. [\[CrossRef\]](#)
10. Wang, G.; Bronson, K.F.; Thorp, K.R.; Mon, J.; Badaruddin, M. Multiple leaf measurements improve effectiveness of chlorophyll meter for durum wheat nitrogen management. *Crop Sci.* **2014**, *54*, 817–826. [\[CrossRef\]](#)
11. Ali, A.M.; Thind, H.S.; Sharma, S.; Singh, Y. Site-specific nitrogen management in dry direct-seeded rice using chlorophyll meter and leaf colour chart. *Pedosphere* **2015**, *25*, 72–81. [\[CrossRef\]](#)
12. Wu, J.; Wang, D.; Rosen, C.J.; Bauer, M.E. Comparison of petiole nitrate concentrations, SPAD chlorophyll readings, and QuickBird satellite imagery in detecting nitrogen status of potato canopies. *Field Crop. Res.* **2007**, *101*, 96–103. [\[CrossRef\]](#)
13. Dordas, C.A. Chlorophyll meter readings, N leaf concentration and their relationship with N use efficiency in oregano. *J. Plant Nutr.* **2017**, *40*, 391–403. [\[CrossRef\]](#)
14. Yuan, Z.; Ata-Ul-Karim, S.T.; Cao, Q.; Lu, Z.; Cao, W.; Zhu, Y.; Liu, X. Indicators for diagnosing nitrogen status of rice based on chlorophyll meter readings. *Field Crop. Res.* **2016**, *185*, 12–20. [\[CrossRef\]](#)
15. Ciganda, V.S.; Gitelson, A.A.; Schepers, J. How deep does a remote sensor sense? Expression of chlorophyll content in a maize canopy. *Remote Sens. Environ.* **2012**, *126*, 240–247. [\[CrossRef\]](#)
16. Wang, J.; Huang, W.; Lao, C.; Zhang, L.; Luo, C.; Wang, T.; Liu, L.; Song, X.; Ma, Z. Inversion of winter wheat foliage vertical distribution based on canopy reflected spectrum by partial least squares regression method. *Guang Pu Xue Yu Guang Pu Fen Xi* **2007**, *27*, 1319–1322.
17. Wang, Z.; Wang, J.; Liu, L.; Huang, W.; Zhao, C.; Lu, Y. Estimation of Nitrogen Status in Middle and Bottom Layers of Winter Wheat Canopy by Using Ground-Measured Canopy Reflectance. *Commun. Soil Sci. Plant Anal.* **2005**, *36*, 2289–2302. [\[CrossRef\]](#)

18. Huang, W.; Wang, Z.; Huang, L.; Lamb, D.W.; Ma, Z.; Zhang, J.; Wang, J.; Zhao, C. Estimation of vertical distribution of chlorophyll concentration by bi-directional canopy reflectance spectra in winter wheat. *Precis. Agric.* **2011**, *12*, 165–178. [[CrossRef](#)]
19. Keating, B.; Wafula, B. Modelling the fully expanded area of maize leaves. *Field Crop. Res.* **1992**, *29*, 163–176. [[CrossRef](#)]
20. Valentinuz, O.R.; Tollenaar, M. Vertical profile of leaf senescence during the grain-filling period in older and newer maize hybrids. *Crop Sci.* **2004**, *44*, 827–834.
21. Ciganda, V.; Gitelson, A.; Schepers, J. Vertical profile and temporal variation of chlorophyll in maize canopy: Quantitative “crop vigor” indicator by means of reflectance-based techniques. *Agron. J.* **2008**, *100*, 1409–1417. [[CrossRef](#)]
22. Kong, W.; Huang, W.; Zhou, X.; Ye, H.; Dong, Y.; Casa, R. Off-nadir hyperspectral sensing for estimation of vertical profile of leaf chlorophyll content within wheat canopies. *Sensors* **2017**, *17*, 2711. [[CrossRef](#)] [[PubMed](#)]
23. Blackburn, G.A. Quantifying chlorophylls and carotenoids at leaf and canopy scales: An evaluation of some hyperspectral approaches. *Remote Sens. Environ.* **1998**, *66*, 273–285. [[CrossRef](#)]
24. Zarco-Tejada, P.J.; Miller, J.R.; Noland, T.L.; Mohammed, G.H.; Sampson, P.H. Scaling-up and model inversion methods with narrowband optical indices for chlorophyll content estimation in closed forest canopies with hyperspectral data. *IEEE Trans. Geosci. Remote Sens.* **2001**, *39*, 1491–1507. [[CrossRef](#)]
25. Vogelmann, J.; Rock, B.; Moss, D. Red edge spectral measurements from sugar maple leaves. *Remote Sens.* **1993**, *14*, 1563–1575. [[CrossRef](#)]
26. Tucker, C.J. Red and photographic infrared linear combinations for monitoring vegetation. *Remote Sens. Environ.* **1979**, *8*, 127–150. [[CrossRef](#)]
27. Gamon, J.; Serrano, L.; Surfus, J. The photochemical reflectance index: An optical indicator of photosynthetic radiation use efficiency across species, functional types, and nutrient levels. *Oecologia* **1997**, *112*, 492–501. [[CrossRef](#)]
28. Gitelson, A.A.; Keydan, G.P.; Merzlyak, M.N. Three-band model for noninvasive estimation of chlorophyll, carotenoids, and anthocyanin contents in higher plant leaves. *Geophys. Res. Lett.* **2006**, *33*, 11. [[CrossRef](#)]
29. Penuelas, J.; Baret, F.; Filella, I. Semi-empirical indices to assess carotenoids/chlorophyll a ratio from leaf spectral reflectance. *Photosynthetica* **1995**, *31*, 221–230.
30. Datt, B. Remote sensing of water content in Eucalyptus leaves. *Aust. J. Bot.* **1999**, *47*, 909–923. [[CrossRef](#)]
31. Sims, D.A.; Gamon, J.A. Relationships between leaf pigment content and spectral reflectance across a wide range of species, leaf structures and developmental stages. *Remote Sens. Environ.* **2002**, *81*, 337–354. [[CrossRef](#)]
32. Dash, J.; Curran, P. The MERIS Terrestrial Chlorophyll Index. *Int. J. Remote Sens.* **2004**, *25*, 5403–5413. [[CrossRef](#)]
33. Daughtry, C.; Walthall, C.; Kim, M.; De Colstoun, E.B.; McMurtrey, J., III. Estimating corn leaf chlorophyll concentration from leaf and canopy reflectance. *Remote Sens. Environ.* **2000**, *74*, 229–239. [[CrossRef](#)]
34. Haboudane, D.; Miller, J.R.; Tremblay, N.; Zarco-Tejada, P.J.; Dextraze, L. Integrated narrow-band vegetation indices for prediction of crop chlorophyll content for application to precision agriculture. *Remote Sens. Environ.* **2002**, *81*, 416–426. [[CrossRef](#)]
35. Main, R.; Cho, M.A.; Mathieu, R.; O’Kennedy, M.M.; Ramoelo, A.; Koch, S. An investigation into robust spectral indices for leaf chlorophyll estimation. *ISPRS J. Photogramm. Remote Sens.* **2011**, *66*, 751–761. [[CrossRef](#)]
36. Lötscher, M.; Stroh, K.; Schnyder, H. Vertical leaf nitrogen distribution in relation to nitrogen status in grassland plants. *Ann. Bot.* **2003**, *92*, 679–688. [[CrossRef](#)]
37. Bertheloot, J.; Martre, P.; Andrieu, B. Dynamics of light and nitrogen distribution during grain filling within wheat canopy. *Plant Physiol.* **2008**, *148*, 1707–1720. [[CrossRef](#)] [[PubMed](#)]
38. Drouet, J.; Bonhomme, R. Do variations in local leaf irradiance explain changes to leaf nitrogen within row maize canopies? *Ann. Bot.* **1999**, *84*, 61–69. [[CrossRef](#)]
39. Shiratsuchi, H.; Yamagishi, T.; Ishii, R. Leaf nitrogen distribution to maximize the canopy photosynthesis in rice. *Field Crop. Res.* **2006**, *95*, 291–304. [[CrossRef](#)]
40. Wu, C.; Niu, Z.; Tang, Q.; Huang, W. Estimating chlorophyll content from hyperspectral vegetation indices: Modeling and validation. *Agric. For. Meteorol.* **2008**, *148*, 1230–1241. [[CrossRef](#)]
41. Li, H.; Zhao, C.; Huang, W.; Yang, G. Non-uniform vertical nitrogen distribution within plant canopy and its estimation by remote sensing: A review. *Field Crop. Res.* **2013**, *142*, 75–84. [[CrossRef](#)]
42. Trawczynski, C. Assessment of the nutrition of potato plants with nitrogen according to the NNI test and SPAD indicator. *J. Elem.* **2019**, *24*, 2. [[CrossRef](#)]
43. Lambert, R.; Johnson, R. Leaf angle, tassel morphology, and the performance of maize hybrids 1. *Crop Sci.* **1978**, *18*, 499–502. [[CrossRef](#)]
44. Azumi, Y.; Watanabe, A. Evidence for a senescence-associated gene induced by darkness. *Plant Physiol.* **1991**, *95*, 577–583. [[CrossRef](#)]
45. Maddonni, G.A.; Otegui, M.E.; Cirilo, A.G. Plant population density, row spacing and hybrid effects on maize canopy architecture and light attenuation. *Field Crop. Res.* **2001**, *71*, 183–193. [[CrossRef](#)]
46. Monsi, M.; Saeki, T. On the factor light in plant communities and its importance for matter production. *Ann. Bot.* **2005**, *95*, 549. [[CrossRef](#)]
47. Ma, D.; Xie, R.; Niu, X.; Li, S.; Long, H.; Liu, Y. Changes in the morphological traits of maize genotypes in China between the 1950s and 2000s. *Eur. J. Agron.* **2014**, *58*, 1–10. [[CrossRef](#)]

-
48. Schlemmer, M.; Gitelson, A.; Schepers, J.; Ferguson, R.; Peng, Y.; Shanahan, J.; Rundquist, D. Remote estimation of nitrogen and chlorophyll contents in maize at leaf and canopy levels. *Int. J. Appl. Earth Obs. Geoinf.* **2013**, *25*, 47–54. [[CrossRef](#)]
 49. Feng, W.; Qi, S.; Heng, Y.; Zhou, Y.; Wu, Y.; Liu, W.; He, L.; Li, X. Canopy vegetation indices from in situ hyperspectral data to assess plant water status of winter wheat under powdery mildew stress. *Front. Plant Sci.* **2017**, *8*, 1219. [[CrossRef](#)] [[PubMed](#)]